



This is a repository copy of *Adhesion of grafted-to polyelectrolyte brushes functionalized with calix[4]resorcinarene and deposited as a monolayer.*

White Rose Research Online URL for this paper:  
<https://eprints.whiterose.ac.uk/170239/>

Version: Accepted Version

---

**Article:**

Seddon, W.D., Alfahid, L., Dunbar, A.D.F. et al. (2 more authors) (2020) Adhesion of grafted-to polyelectrolyte brushes functionalized with calix[4]resorcinarene and deposited as a monolayer. *Langmuir*, 36 (46). pp. 13843-13852. ISSN 0743-7463

<https://doi.org/10.1021/acs.langmuir.0c02236>

---

This document is the Accepted Manuscript version of a Published Work that appeared in final form in *Langmuir*, copyright © American Chemical Society after peer review and technical editing by the publisher. To access the final edited and published work see <https://doi.org/10.1021/acs.langmuir.0c02236>

**Reuse**

Items deposited in White Rose Research Online are protected by copyright, with all rights reserved unless indicated otherwise. They may be downloaded and/or printed for private study, or other acts as permitted by national copyright laws. The publisher or other rights holders may allow further reproduction and re-use of the full text version. This is indicated by the licence information on the White Rose Research Online record for the item.

**Takedown**

If you consider content in White Rose Research Online to be in breach of UK law, please notify us by emailing [eprints@whiterose.ac.uk](mailto:eprints@whiterose.ac.uk) including the URL of the record and the reason for the withdrawal request.



[eprints@whiterose.ac.uk](mailto:eprints@whiterose.ac.uk)  
<https://eprints.whiterose.ac.uk/>

## Title

Adhesion of grafted-to polyelectrolyte brushes functionalized with calix[4]resorcinarene and deposited as a monolayer

## Author List

William D. Seddon,<sup>\*,†,‡</sup> Latifah Alfahid,<sup>‡</sup> Alan D. F. Dunbar,<sup>§</sup> Mark Geoghegan,<sup>‡</sup> and Nicholas H. Williams<sup>†</sup>

<sup>†</sup>Department of Chemistry, University of Sheffield, Brook Hill, Sheffield S3 7HF, U.K.

<sup>‡</sup>Department of Physics and Astronomy, University of Sheffield, Hicks Building, Hounsfield Road, Sheffield S3 7RH, U.K.

<sup>§</sup>Department of Chemical and Biological Engineering, University of Sheffield, Sir Robert Hadfield Building, Mappin Street, Sheffield S1 3JD, U.K.

## Abstract

Polyelectrolyte adhesives, either poly[2-(dimethylamino)ethyl methacrylate] or poly(methacrylic acid), functionalized with a surface-active calix[4]resorcinarene were grafted onto silicon wafers. Adhesion studies on these grafted-to brushes using polyelectrolyte hydrogels of opposite charge showed that it is the calix[4]resorcinarene, rather than adsorption of polyelectrolyte monomers, that adheres the brush to the silicon substrate. The adhesion measured was similar to that measured using polymers grafted-from the surface, and was stronger than a control layer of poly(vinyl acetate) under the same test conditions. The limiting factor was determined to be adhesive failure at the hydrogel-brush interface, rather than the brush-silicon interface. Therefore, the adhesion has not been adversely affected by changing from a grafted-from to a grafted-to brush, demonstrating the possibility of a one-pot approach to creating switchable adhesives.

## Introduction

Calixarenes<sup>1–5</sup> are bowl-shaped molecules that can be used to form monolayers on surfaces with controlled orientation due to the hydrophilic nature of the hydroxyls on the upper rim, or via chemical functionalization of the upper or lower rim.<sup>6–9</sup> This capacity for modification also allows additional functionality to be introduced to a surface or solution.<sup>1,3,6,7,9–11</sup> One potential use of this functionalization is to deliver an adhesive to a surface of interest. In this work, polyelectrolytes, with a view to switchable adhesion applications,<sup>12–16</sup> were delivered to surfaces utilizing the monolayer capacity of calixarene and its hydroxyl rich rim.

Initial work using an end-grafted polycation and a polyanionic hydrogel<sup>14</sup> demonstrated the viability of polyelectrolyte switchable adhesion, but the adhesive strength was limited by cohesive failure of the hydrogel, which resulted in the gel splitting and leaving material still adhered to the surface when the adhesive bond strength was greater than the mechanical strength of the hydrogel. This was improved<sup>15</sup> through the use of double-network hydrogels. The secondary network increases the fracture resistance of the polyanionic hydrogel, which would otherwise be brittle,<sup>17</sup> increasing the maximum adhesive bond strength.

A limiting factor on these adhesives, and many other smart adhesives, is the requirement for complex chemistry to prepare the adhesive *in situ*. In the case of these adhesives, they are prepared as polyelectrolyte brushes on the surface using a grafting-from technique. Preparation of these polymers on the surface is not trivial, and requires the use of reactive chemicals, metal catalysts, and both anhydrous and deoxygenated conditions over the course of the synthesis.<sup>14–16,18–20</sup> Although this is achievable in a laboratory environment on a relatively small scale, this process would be difficult

to translate to large components or a commercial environment. In order to move switchable adhesives towards commercial applications, any requirement for the end user to perform any chemistry should be removed. Ideally, the adhesive coatings would be prepared *ex situ* and applied where needed in a ‘one-pot’ approach.

In order to move towards this goal, polyelectrolyte adhesives have here been developed from a laboratory grafting-from technique towards a grafting-to technique where coating material can be directly applied to the desired surface. The surface delivery and peak adhesion of the grafted-to coating was investigated to determine the viability of this route and compared to similar materials prepared by grafting-from methods.

Switchable or reversible adhesives bond and de-bond in response to an external, controllable, stimulus.<sup>21</sup> This offers the capacity to disassemble components without causing damage to the substrates, and has proved useful in areas such as painless wound dressings,<sup>22,23</sup> end-of-life decommissioning and recycling,<sup>24,25</sup> and microrobotics.<sup>26–28</sup> Smart adhesives are generated through the introduction of physical or chemical functionality. As an example of the former, topographical adhesives have their adhesive strength altered by maximizing and minimizing the degree of contact area in a reversible process.<sup>29</sup> They have been developed to respond to a variety of stimuli, including temperature,<sup>30,31</sup> magnetic and electric fields,<sup>27,32–34</sup> and mechanical.<sup>35–37</sup> Controlling adhesion through chemical functionality involves manipulating molecular interactions. Materials have been developed to respond to a variety of stimuli, including temperature,<sup>22,38</sup> light,<sup>24,30,38,39</sup> solvent,<sup>40</sup> and pH,<sup>23,41</sup> although some are ineffective in aqueous environments.<sup>25,42</sup> There are very few examples where self-assembly of the adhesives is demonstrated, a property that is used in the present work. Indeed, only one of the above examples makes use of self-assembly behavior.<sup>30</sup>

For this work, calix[4]resorcinarene was selected to provide an anchoring group from which the polyelectrolyte adhesives could be grown prior to deposition. The well-defined molecular structure of calix[4]resorcinarene provides a useful molecular framework that allows the polyelectrolyte to be orientated away from the surface by using the lower rim. Calix[4]resorcinarene was modified with either poly[2-(dimethylamino)ethyl methacrylate] (pDMAEMA) or poly(methacrylic acid) (pMAA) and deposited on (grafted-to) hydrophobically modified silicon wafers using Langmuir-Schaefer deposition to generate a dense monolayer of adhesive (Figure 1). The deposited material was tested for adhesiveness using hydrogels of oppositely charged polyelectrolytes. The results were then compared to previous work using polyelectrolytes grown directly from the surface.<sup>14,15,18–20,43</sup> These grafted-from adhesives have been shown to display strong adhesion which can be switched reversibly over multiple cycles by utilizing changes in pH.<sup>15,18</sup> This repeatable nature makes them useful candidates for applications where components need to be reassembled.

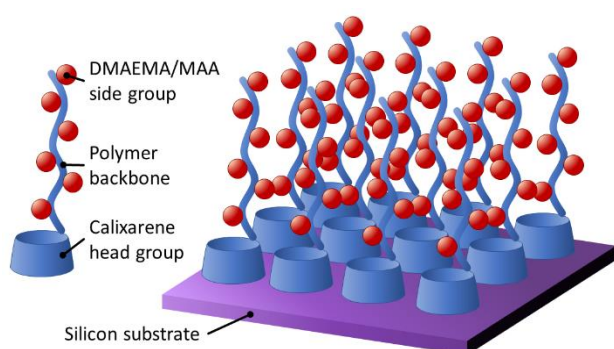


**Figure 1:** Schematic illustration of the deposited adhesive layer.

A model system is investigated here, with a flat silicon wafer as the substrate, and milli-Q ultra-pure water as the medium for adhesion experiments. This enables a fundamental evaluation of the grafted-to adhesive and allow a more direct comparison to previous work. In real-world applications, the adhesive would be applied to more diverse

substrates, using the ability of calixarenes to adhere to various surfaces, with further modification to tailor substrate adhesion also possible.<sup>6,7</sup> Testing these adhesives on such diverse substrates is beyond the scope of this initial study. The current system performs well on flat surfaces, and the relatively high surface roughness and presence of asperities on real-world surfaces may restrict its broader application at present. Although not investigated as part of this study, when grafted-from a surface these polyelectrolytes have been shown to demonstrate reversible and repeatable adhesion by changing the pH of the solution in contact with the adhesive interface.<sup>15,16,20</sup> Increases in the salt concentration of the solution can also be used to reverse the adhesion through charge screening.<sup>43,44</sup> However, the concentration required to achieve this is much higher than would be encountered in tap water conditions, so adhesion couples such as those described here can be tailored to work in diverse aqueous systems.

## Experimental Section

### Materials

Solvents and reagents were purchased from commercial sources and used directly without purification unless noted otherwise. Anhydrous solvents were obtained from a Grubbs solvent apparatus. Copper(I) Bromide (Cu<sup>I</sup>Br) was purified by sequential washing with glacial acetic acid, ethanol, and diethyl ether, and was oven dried and kept under nitrogen.<sup>45</sup> Mono-C-decenyl, tri-C-decyl calix[4]resorcinarene and C-decyl calix[4]resorcinarene (**1** & **2**);<sup>46</sup> Boc-mono-C-decenyl, tri-C-decyl calix[4]resorcinarene and Boc-C-decyl calix[4]resorcinarene (**3** & **4**);<sup>47</sup> and Boc-mono-C-decanol, tri-C-decyl calix[4]resorcinarene (**5**)<sup>46</sup> were prepared as previously described. The full preparation of the poly[2-(diethylamino)ethyl methacrylate] (pDEAEMA)<sup>16</sup> and double-network poly(methacrylic acid)-poly[oligo(ethylene glycol) methyl ether methacrylate] (DN pMAA-pOEGMA) hydrogels<sup>15,43</sup> is described in the supporting information. Briefly, the hydrogels were formed by placing the reaction mixture in a sealable glass container containing a mold with hemispherical holes of 4 mm diameter. This glass container was placed in an oven until the polymerization was complete, and the resulting gel cut into individual hemispherical pieces and stored in deionized water until use. The double network hydrogels were then immersed in a second reaction mixture for 5 days, then removed and placed in the glass container in the oven, polymerized, and stored as before. Additional experimental details, including full synthetic procedures, are given in the supporting information.

### Synthesis of the polyelectrolyte adhesives

Calix[4]resorcinarene was covalently tethered to either pDMAEMA or pMAA to give the calix[4]resorcinarene adhesives **7**, **8**, and **10** (Figure 2). Control compounds where the calix[4]resorcinarene is replaced by a decyl group to give decyl-pDMAEMA **12** and decyl-pMAA **14** (Figure 2) were also synthesized.

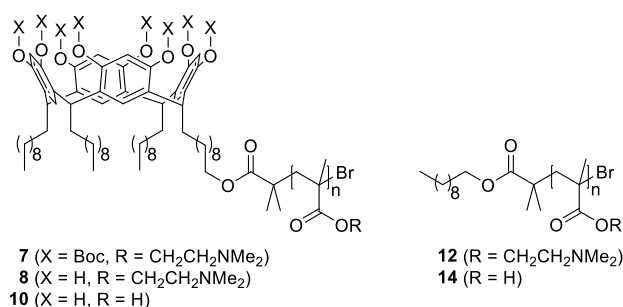


**Figure 2:** Calixarene adhesives **7**, **8**, and **10**, and decyl controls **12** and **14**.

The overall synthetic route for the calix[4]resorcinarene adhesives **8** and **10** is shown in Figure 3. To be able to connect each polyelectrolyte chain to its own surface anchor, a monofunctional calixarene was prepared via the statistical

incorporation of differing aldehydes, giving a mixture of mono- and unfunctionalized lower rim calix[4]resorcinarenes.<sup>46</sup> *Tert*-butoxycarbonyl (Boc) protection followed by hydroboration-oxidation gave Boc-mono-*C*-decanol, tri-*C*-decyl calix[4]resorcinarene **5**.<sup>46,47</sup>

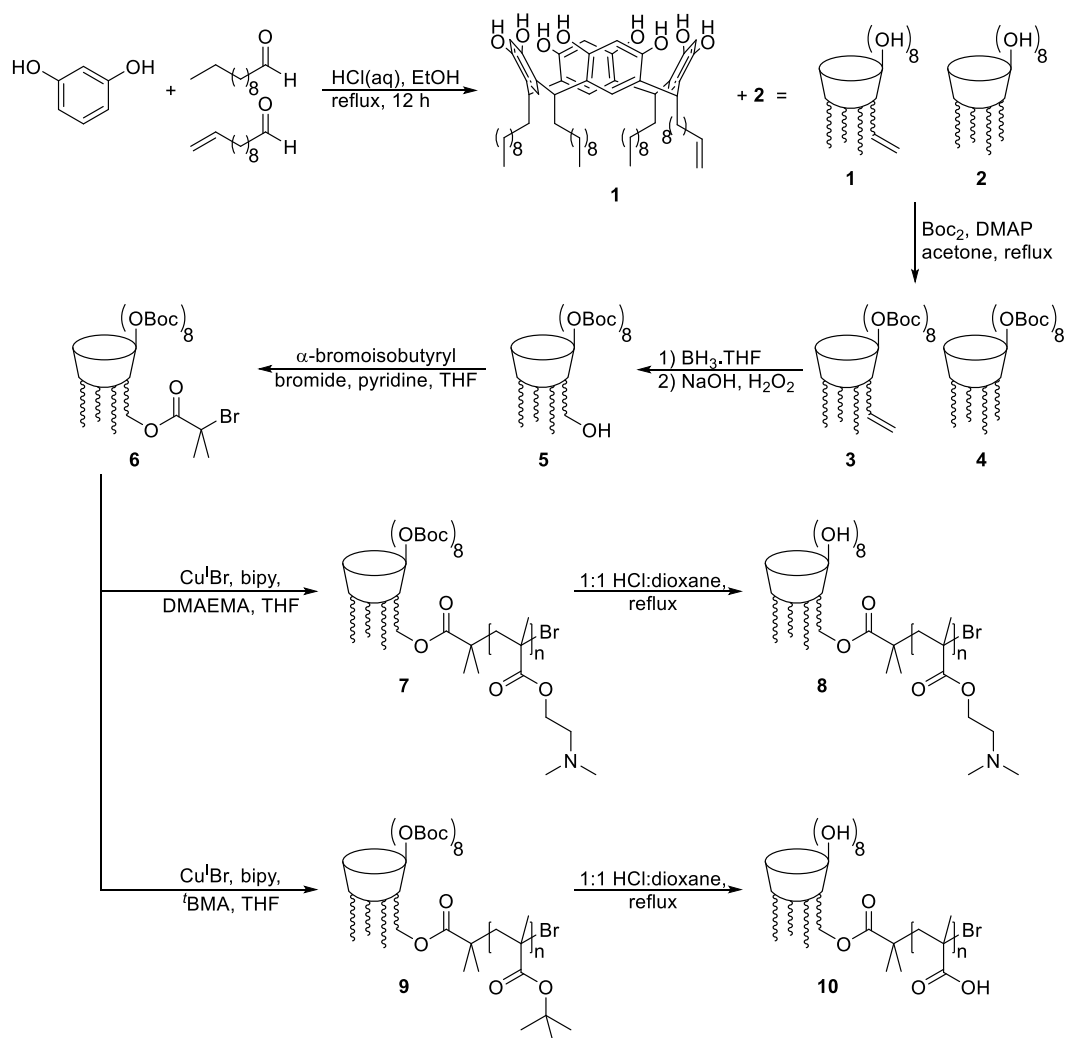


**Figure 3:** Synthetic route for the calix[4]resorcinarene adhesives **7**, **8**, and **10**.

An ATRP initiator was attached to mono-hydroxyl calix[4]resorcinarene **5** using α-bromoisobutyryl bromide and pyridine in anhydrous tetrahydrofuran (THF), which gave the Boc-calix[4]resorcinarene bromoinitiator **6** after purification by chromatography. Boc-calix[4]resorcinarene bromoinitiator **6** was used to polymerize 2-(dimethylamino)ethyl methacrylate to give the polybase Boc-calix[4]resorcinarene-pDMAEMA **7** using ATRP. Once the polymer had been prepared, the Boc protecting groups were removed to reveal the phenolic hydroxyls on the upper rim. Acidic cleavage using HCl/dioxane gave the deprotected calix[4]resorcinarene-pDMAEMA **8**.<sup>48</sup> Both the Boc protected and Boc deprotected materials **7** and **8** have the potential to be used as adhesives, as the hydrophobic *tert*-butyl groups of Boc will also interact with the hydrophobic wafers.

*Tert*-butyl methacrylate (<sup>t</sup>BMA) was used as a protected monomer to give Boc-calix[4]resorcinarene-p<sup>t</sup>BMA **9**.<sup>49</sup> Boc-calix[4]resorcinarene-p<sup>t</sup>BMA **9** was then deprotected by acid hydrolysis to yield the polyacid adhesive calix[4]resorcinarene-pMAA **10**. The acid deprotection also removes the Boc protecting groups from the calix[4]resorcinarene bowl. This dual deprotection meant that it was not possible to prepare Boc-calix[4]resorcinarene-pMAA adhesive in addition to calix[4]resorcinarene-pMAA **10**.

Control compounds were also required to demonstrate that the calix[4]resorcinarene has a specific effect upon surface adherence and the overall adhesion of the system. In addition to the calix[4]resorcinarene based adhesives **7**, **8**, and **10**, control compounds using decane instead of calix[4]resorcinarene were prepared using the same synthetic methods to give decyl-pDMAEMA **12** and decyl-pMAA **14** (Figure 4). The decyl group is analogous to the pendant chains from the lower annulus of a calix[4]resorcinarene, but lacks the surface attachment or molecular framework capabilities of the calix[4]resorcinarene bowl.

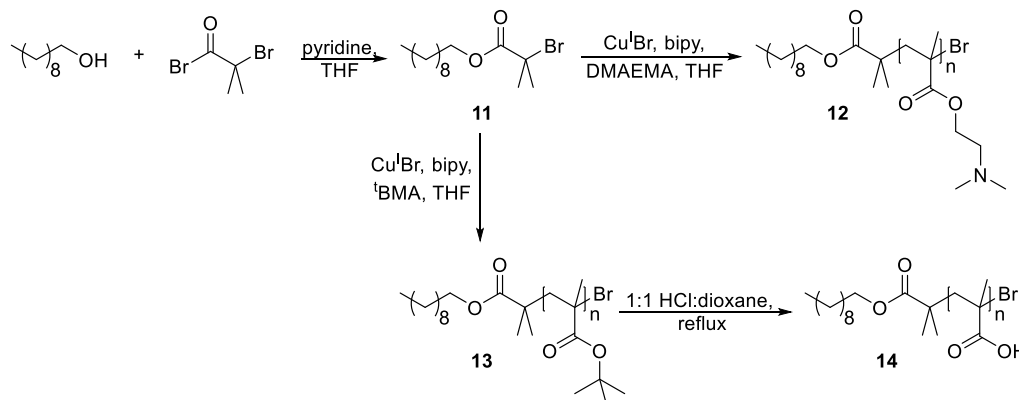


**Figure 4:** Synthetic route for the decyl controls **12** and **14**.

To provide comparison with traditional adhesives, thin films of poly(vinyl acetate) (PVAc) were prepared by spin coating from toluene to provide films of a similar thickness ( $12.7 \pm 0.5$  nm) to the deposited calixarene adhesives.

### Preparation of silicon wafers

Silicon wafers were purchased from Prolog Semicon Ltd with the following characteristics: diameter 50.8 mm (2"), dopant p-type boron, orientation  $(100) \pm 1^\circ$ , resistivity 0-0.3  $\Omega\text{m}$ , thickness  $275 \pm 25$   $\mu\text{m}$ . Wafers were either used whole or cut to size ( $\sim 12 \times 15$  mm). Wafers were cleaned and rendered hydrophilic using piranha solution (3:1 sulfuric acid:hydrogen peroxide). Once the solution had cooled, the wafer samples were washed repeatedly with deionized water and oven dried.

Hydrophobic wafers were prepared by treating piranha solution cleaned wafers with hexamethyldisilazane (HMDS). Clean wafers were placed in a sealed sample tube with three drops of HMDS and heated to  $80^\circ\text{C}$  for 15 min. Once the wafers had cooled, they were rinsed in toluene and then dried under a stream of compressed air.

PVAc coated surfaces were prepared by spin coating. The surface of a piranha cleaned wafer was flooded with poly(vinyl acetate) ( $M_w = 50$  kg mol<sup>-1</sup>) dissolved in toluene (87  $\mu\text{M}$ ), then spun at 4500 rpm for 60 seconds.

### Langmuir-Schaefer film preparation

The calix[4]resorcinarene based adhesives were designed to allow a grafting-to method to be used to connect an adhesive monolayer to surfaces in a one-pot procedure by forming a single polyelectrolyte adhesive monolayer. This is in contrast to current grafting-from approaches, where the adhesive monolayer is generated on the surface through the use of synthetically intensive methods. Langmuir-Schaefer deposition of the calix[4]resorcinarene-based adhesives was used to prepare the films rather than spontaneous assembly from solution because it provided quantitative and reproducible information on the monolayer so formed.

Langmuir films of the calix[4]resorcinarene adhesives **7**, **8**, and **10**, and decyl controls **12** and **14** were formed using a Langmuir trough (601BAM, NIMA Technology). Pressure control was set to either 40 mN m<sup>-1</sup> for calixarene adhesives **7**, **8**, and **10**, or 35 mN m<sup>-1</sup> for decyl control compounds **12** and **14**. Langmuir-Schaefer depositions were performed using a dipper mechanism (D1L, NIMA Technology), controlled by a Tacho speed control (model TSC7), and a micro-processor interface (IU4, NIMA Technology). All samples were spread on a pH6 Milli-Q water subphase, with the polyelectrolyte chains dissolved in the subphase and the calixarene bowls in the air phase, and transferred by the Langmuir-Schaefer technique (horizontal stamping from above) onto hydrophobically modified silicon wafers (pre-treated with hexamethyldisilazane, HMDS). Hydrophobic wafers were brought into contact with the trough surface using the dipper arm with a speed of 35 mm min<sup>-1</sup> and withdrawn with the same speed. The samples were dried using a stream of compressed air. Additional samples were also either post-baked in an oven at 100 °C for 15 min or sonicated in Milli-Q water for 15 min and dried using a stream of compressed air.

The thickness of deposited material was determined using a M-2000V Rotating Compensator Ellipsometer (J. A. Woollam Co.) and CompleteEASE software for data fitting. The deposited films were modelled as a uniform material on a silicon substrate, and fitted using a B-Spline model for the film. The native oxide with HMDS coating on the silicon substrates was measured separately, and subtracted from the total film thickness to give the brush layer thickness. Multiple measurements were taken across the surface of each sample, the results averaged, and the standard error determined. The total thickness of the native oxide and HMDS coating was 1.5 ± 0.1 nm.

## Adhesion measurements

Adhesion measurements were performed using a Texture Analyser TA.XTplus (Stable Microsystems), which brought a hemispherical hydrogel of the opposite charge into contact with the sample surface using a standard protocol. The surface and the hydrogel probe were immersed in Milli-Q water for the duration of the experiment. The gel was brought towards the polyelectrolyte film using an approach speed of 50 mm min<sup>-1</sup>. Upon contact a pressure of 0.5 N was applied for 2 min, before the gel was withdrawn at a constant speed of 50 mm min<sup>-1</sup>. A DN pMAA-pOEGMA hydrogel was used for calix[4]resorcinarene adhesives **7** and **8**, and decyl control **12**. Double-network hydrogels consist of a primary network of crosslinked polymer, in this case pMAA, reinforced with a secondary network of a different polymer with a lower degree of crosslinking, in this case pOEGMA. This secondary network increases the fracture resistance of the pMAA hydrogel.<sup>17</sup> A pDEAEMA hydrogel was used for calix[4]resorcinarene adhesive **10** and decyl control **14**. Results were processed using Exponent software (Stable Microsystems). Side-view images of the interface were taken using a camera, Stable Microsystems, and the images processed using ImageJ to determine contact diameter and height. The average contact area of the DN pMAA-pOEGMA hydrogel under compression was 17.1 ± 0.1 mm<sup>2</sup> for the first measurements, and 18.2 ± 0.3 mm<sup>2</sup> for the repeat measurements. The average contact area of the pDEAEMA hydrogel under compression was 23.7 ± 0.6 mm<sup>2</sup> for the first measurements, and 27.7 ± 0.7 mm<sup>2</sup> for the repeat measurements.

## Results and Discussion

### Characterization of the deposited surfaces

The thickness of the deposited materials was determined using spectroscopic ellipsometry, and the results are summarized in Figure 5. Calix[4]resorcinarene adhesives **7** and **8**, and decyl-pDMAEMA control **12** showed resistance to the post deposition treatments that were used. The post deposition bake had no significant effect upon the thickness, showing that there was no contribution from absorbed water in swelling the polymer film, and the water sonication showed that the films were resistant to desorption, with the small increase in thickness attributable to swelling from

absorbed water. Calix[4]resorcinarene-pMAA **10** showed a greater change with post treatment. The water sonication showed a reduction in film thickness, indicating either a loss of material from the surface, or a reorganization of the tethered polymer.

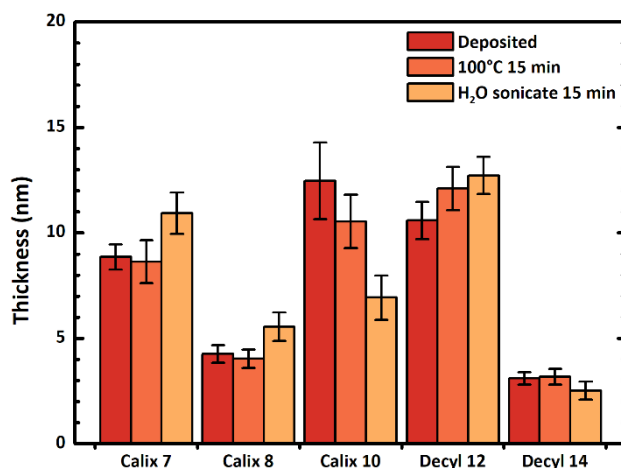


**Figure 5:** Deposited film thickness of calix[4]resorcinarene adhesives **7**, **8**, and **10**, and decyl controls **12** and **14** deposited by Langmuir-Schaefer deposition. The thickness was measured using ellipsometry and accounted for the native oxide and HMDS coating.

The grafting density<sup>50</sup> ( $\sigma$ ),  $\sigma = (l\rho_{\text{pol}}N_A)/M_n$  ( $l$ , thickness of the brush;  $\rho_{\text{pol}}$ , density of the polymer;<sup>50,51</sup>  $N_A$ , Avogadro's number; and  $M_n$ , number average molecular weight); radius of gyration<sup>52,53</sup> ( $R_g$ ),  $R_g = \sqrt{Nb^2/6}$  ( $b$ , segment length;<sup>55,56</sup> and  $N$ , number of methacrylate monomer units); interchain distance<sup>54</sup> ( $D$ ),  $D = \frac{1}{\sqrt{\sigma}}$ ; and reduced tether density<sup>55</sup> ( $\Sigma$ ),  $\Sigma = \sigma\pi R_g^2$ , of the deposited films were calculated from the measured thickness and chain lengths,<sup>50,52–55</sup> and are listed in Table 1. Using the reduced tether density (the number of chains per area that would be filled by untethered non-overlapping chains under the same conditions), the polymer film can be characterized by three conformational regimes: the ‘mushroom’ or weakly interacting regime at  $\Sigma < 1$ ; the mushroom to brush transition regime at  $1 < \Sigma < 5$ ; and the brush regime at  $\Sigma > 5$ .<sup>55</sup> All the deposited materials apart from decyl-pMAA **14** have an interchain distance either equal to or less than the radius of gyration of the polymer in solution, and consequently are in a brush or brush-like regime. The reduced tether densities for **8** and **10** indicate that they are in the mushroom to brush transition regime, and the reduced tether densities for **7** and **12** indicate that they are in the ‘true’ brush regime.

A calix[4]resorcinarene bowl has a diameter between 1-1.32 nm,<sup>56</sup> and therefore an area of 0.79-1.37 nm<sup>2</sup>, giving a maximum grafting density of 0.73-1.27 nm<sup>-2</sup>. Calix[4]resorcinarene-pMAA **10** has a grafting density within this maximum grafting density of calix[4]resorcinarene, indicating that the calix[4]resorcinarene is the limiting factor for this polymer film, rather than the polymer.

**Table 1:** Compounds deposited from solution showing thickness, number of chain units ( $N$ ), radius of gyration ( $R_g$ ), grafting density ( $\sigma$ ), interchain distance ( $D$ ), and reduced tether density ( $\Sigma$ ).

Compound	As-deposited thickness (nm)	$N$	$R_g$ (nm)	$\sigma$ (nm <sup>-2</sup> )	$D$ (nm)	$\Sigma$
Calix <b>7</b>	8.9 ± 0.6	82	2	0.55 ± 0.04	1.35 ± 0.03	6.9 ± 0.5
Calix <b>8</b>	4.3 ± 0.4	82	2	0.27 ± 0.03	1.92 ± 0.05	3.4 ± 0.3
Calix <b>10</b>	12 ± 2	85	1	1.1 ± 0.2	0.95 ± 0.07	3.1 ± 0.5

Decyl <b>12</b>	10.6 ± 0.9	82	2	0.64 ± 0.05	1.25 ± 0.04	8.0 ± 0.7
Decyl <b>14</b>	3.0 ± 0.3	85	1	0.28 ± 0.03	1.89 ± 0.05	0.79 ± 0.07

### AFM imaging of deposited brushes

The surface roughness and topography of the deposited materials were determined using Atomic Force Microscopy (Asylum MFP-3D AFM, Bruker). The height images for the deposited, the post-baked, and water sonicated surfaces are shown in Figures S5, S6, and S7, respectively. The surface roughness of the HMDS treated wafer and deposited brushes are listed in Table 2.

The HMDS surface was observed to have numerous regular features, rather than a smooth continuum, leading to the observed surface roughness (Figure S5a). These features have an average diameter of  $190 \pm 10$  nm, and an average height of  $4.6 \pm 0.8$  nm, and are attributed to a build-up of the HMDS silanizing agent on the surface. However, the overall effect of the HMDS treatment rendered the wafers hydrophobic, as determined by contact angle goniometry ( $\theta \geq 90^\circ$ ).

**Table 2:** Surface roughness ( $R_a$ ) of the HMDS treated wafers and deposited adhesives.

Compound	$R_a$ (nm)		
	As-deposited	100°C post bake	H <sub>2</sub> O sonicate
<i>HMDS</i>	$0.88 \pm 0.05$	-	-
Calix <b>7</b>	$0.26 \pm 0.03$	$0.31 \pm 0.01$	$0.38 \pm 0.07$
Calix <b>8</b>	$0.72 \pm 0.07$	$0.77 \pm 0.02$	$0.41 \pm 0.05$
Calix <b>10</b>	$0.6 \pm 0.1$	$1.2 \pm 0.1$	$0.40 \pm 0.07$
Decyl <b>12</b>	$0.49 \pm 0.01$	$0.36 \pm 0.01$	$0.64 \pm 0.02$
Decyl <b>14</b>	$1.64 \pm 0.07$	$1.15 \pm 0.02$	$1.34 \pm 0.06$

The deposited Boc-calix-pDMAEMA **7** surfaces (Figure S5b) were observed to have a uniform surface, with the HMDS features almost completely masked by the deposited brush. The hydrophobic head group of this calixarene can adhere to these features in addition to the wafer surface, generating the uniform surface. This is shown across all three surface post treatments (Figures S6a & S7a), and is reflected in the low surface roughness for the films. In contrast, the calix-pDMAEMA **8** surface (Figure S5c) shows a translation on the HMDS features to the brush surface as a series of ‘holes’ in the surface topography, with a measured diameter of  $210 \pm 20$  nm, and a depth of  $4.0 \pm 0.5$  nm. The calixarene head group of calix **8** is more hydrophilic, reducing the ability of the head group to adhere to the HMDS features, leading to the brush preferentially ‘back-filling’ the area between the HMDS features. As the brush height is much smaller than the feature diameter ( $4.3 \pm 0.4$  nm and  $190 \pm 10$  nm, respectively), the features appear as voids in the brush layer, as the conformation of the brushes cannot sufficiently adjust to accommodate the features, and this is reflected in the overall surface roughness of the deposited and post-baked surfaces (Table 2).

The deposited calix-pMAA **10** surfaces (Figure S5d) were also observed to have the small voids related to the HMDS features, and an additional number of larger irregular voids ( $165 \pm 5$  nm). There is a build-up of material around

the edge of these larger voids, which is attributed to film defects. The post-bake treatment (Figure S6c) resulted in a large increase in the surface roughness (Table 2) and the number of larger voids observed. However, the water sonication (Figure S7c) resulted in a reduction in the surface roughness, and the disappearance of the voids, suggesting a re-ordering of the surface.

The control compound decyl-pDMAEMA **12** (Figure S5e) also showed a number of larger voids in the brush layer ( $550 \pm 70$  nm). These are attributed to film defects formed during the Langmuir compression, as the Langmuir film was less stable and prone to buckling at high compression. In the decyl-pMAA **14** surfaces (Figures S5f, S6e, S7e) the overall film coverage is low, with large areas left uncovered, resulting in a large surface roughness (Table 2). This is reflected in the reduced tether density (Table 1) and overall film thickness (Figure 5), and is also attributed to film defects formed during the Langmuir compression.

### Adhesion measurements using polyelectrolyte hydrogels

The deposited materials were tested for adhesion in an aqueous environment using a mechanical tester fitted with a hemispherical hydrogel of the opposite charge. The adhesion force ( $F_a$ ) and the work done ( $W$ ) are shown in Figure 6. For this system, the adhesion force is the maximum value on the force-distance curve and the work done is the energy transferred when the hydrogel is displaced by the adhesive force.

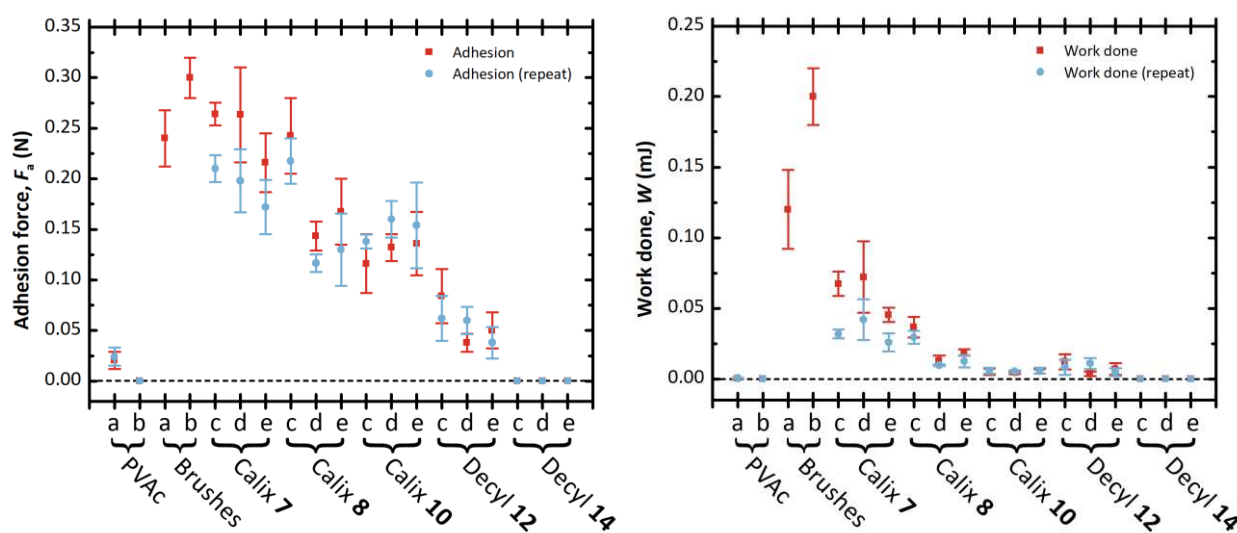


**Figure 6:** Adhesion force and work done of PVAc, previous grafted-from brushes,<sup>15,16</sup> calix[4]resorcinarene adhesives, and decyl controls. Measurements were conducted in pH6 Milli-Q water using pDEAEMA and DN pMAA-pOEGMA hydrogels. The applied load is 0.5 N with a contact time of 2 min. The speed of approach and retraction of the hydrogel probe is  $50 \text{ mm min}^{-1}$ . a) Adhesion with DN pMAA-pOEGMA hydrogel. b) Adhesion with pDEAEMA hydrogel. c) As-deposited samples. d)  $100^\circ\text{C}$  Post-baked samples. e)  $\text{H}_2\text{O}$  sonicated samples.

It was found that the calixarene-based adhesives showed a stronger adhesive response compared to the decyl control compounds. This suggests that the calixarene anchors the adhesive to the surface better than the decyl group, and that it is the presence of the surface-active group, rather than the formation of an ordered monolayer, which is providing the majority of the adhesion of the polyelectrolyte to the surface. The adhesive response was also larger than the spin-coated PVAc surface under the same test conditions. This shows that it is the presence of the polyelectrolyte brush, and its interactions with the polyelectrolyte gel, that is causing the adhesion, rather than the presence of a polymer film.

The surface post-deposition treatments (post-baked at  $100^\circ\text{C}$  or water sonication) in general caused a slight reduction in the measured adhesive strength of the surfaces. The greatest reduction was observed for calix **8**, which may

be due to its thinner film thickness. Calix **10** does not display reduced adhesion with post treatment, despite a reduction in film thickness with water sonication. This reduced film thickness may be due to re-organization of the film rather than loss of material, as suggested by AFM imaging and roughness measurements. All of the post-treated surfaces still displayed similar adhesion to the initial 'as-deposited' surfaces, indicating that these surfaces are resistant to harsher conditions and are still capable of adhesion.

Although there was a decrease in the adhesion observed when the measurements were repeated using the same hydrogel on a different part of the surface for most samples, this decrease was relatively small. This shows that the majority of the measured adhesion was due to adhesive failure at the gel-brush interface, rather than the brush-wafer interface. This means that the limiting factor in this system is the polyelectrolyte adhesion, and not the method of attachment of the polymer to the surface.

The film thickness is not the dominant factor in the adhesive response of the deposited films, as brushes with similar thicknesses (such as calix **7** and decyl **12**) have different adhesive responses which are more affected by the tethering chemistry. Only calix **8** showed a potential impact of relative film thickness on adhesive response as mentioned earlier. However, polyelectrolyte brushes have been shown to have an increased adhesive response with increasing film thickness,<sup>16</sup> so at thicker film thicknesses these deposited films could be expected to have a greater adhesive strength.

The adhesion of the calixarene-based adhesives **7** and **8** ( $0.26 \pm 0.01$  N and  $0.24 \pm 0.05$  N) compares favorably with the previously reported grafted-from brush under the same experimental conditions ( $0.24 \pm 0.03$  N).<sup>15</sup> However, the work done is less than that for the grafted-from brush, so the adhesion acts over a shorter distance, and less energy is required to separate the gel from the brush. This is most likely to be due to the shorter length of the deposited brushes ( $8.9 \pm 0.6$  nm for Calix **7** and 70-80 nm for the grafted-from brush), as this affects the degree of interdigitation into the hydrogel, and the overall strength of the adhesive bond.<sup>16</sup> The adhesion force and work done of calix **10** is smaller than the previously reported grafted-from brush,<sup>16</sup> and again is likely to be due to the shorter length of the deposited brushes ( $12 \pm 2$  nm for Calix **11** and  $32.2 \pm 0.2$  nm for the grafted-from brush).

The stress measured for this system represents the force per unit area that occurs during the removal of the hydrogel, and the strain is due to the deformation caused during separation.<sup>57</sup> From this, if an adhesive joint is behaving elastically, then the dissipation of energy is likely to be through interface separation, with stiffer joints displaying greater elastic moduli. If the adhesive joint is undergoing plastic deformation, then at least a portion of the energy dissipation will be through dissipation in the hydrogel.

The maximum stress and maximum strain are shown in Figure 7. The resultant elastic moduli are shown in Figure S8. The stresses observed are not particularly large, and are similar to those reported previously for these hydrogel systems.<sup>14</sup> The strains are also consistent with prior reports, and reflect the deformable nature of the hydrogel. The smaller stress-strain characteristic observed for the PVAc material can be attributed to the much smaller adhesion between the gel and the polymer film.

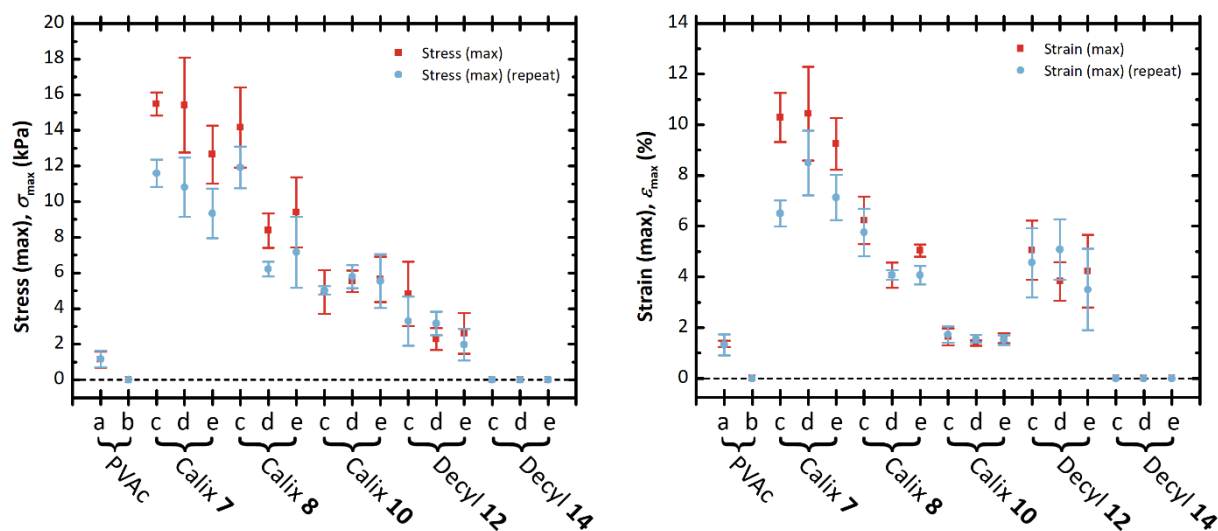


**Figure 7:** Stress (max) and strain (max) of PVAc, calix[4]resorcinarene adhesives, and decyl controls. Measurements were conducted in pH6 Milli-Q water using pDEAEMA and DN pMAA-pOEGMA hydrogels. The applied load is 0.5 N with a contact time of 2 min. The speed of approach and retraction of the hydrogel probe is 50 mm min<sup>-1</sup>. a) Adhesion with DN pMAA-pOEGMA hydrogel. b) Adhesion with pDEAEMA hydrogel. c) As-deposited samples. d) 100 °C Post-baked samples. e) H<sub>2</sub>O sonicated samples.

Although the data here are insufficient for quantitative analysis of the stress-strain characteristics of these adhesive joints, a qualitative discussion of the probable dissipation mechanisms can be presented. The data suggest that for calix 7, calix 8, decyl 12, and PVAc (with the DN pMAA-pOEGMA hydrogel) a portion of the energy dissipation is through deformation of the hydrogel, resulting in a more flexible joint. Conversely, the data suggest that calix 10 showed the opposite: the energy dissipation was primarily through interface separation, resulting in a stiffer joint. The reason for the difference is predominantly down to the differing strengths of the adhesive bond. Calix 10 has a much smaller adhesive strength and so the energy required to break the adhesion is smaller than the energy required to deform the hydrogel irreversibly, which means that the adhesive bond broke before irreversible deformation could occur.

The work of debonding ( $W_{\text{deb}}$ ) is shown in Figure 8. For this system, the work of debonding is the energy required per unit area to separate the hydrogel from the brush surface. It is determined from the area under the stress-strain curve multiplied by the height of hydrogel in contact,  $W_{\text{deb}} = h_0 \int_0^{\varepsilon_{\text{max}}} \sigma(\varepsilon) d\varepsilon$  ( $\sigma$ , stress;  $\varepsilon$ , strain;  $h_0$ , height of hydrogel in contact).<sup>57</sup> The initial measurement has a larger work of debonding than subsequent measurements. The work of debonding for calix 8 is less than that for calix 7, despite having similar adhesion forces. This reduction in the bonding energy is due to the smaller strain observed for these surfaces, meaning the adhesion acts over a shorter distance, and less energy is required to separate the gel from the brush, similar to the work done.

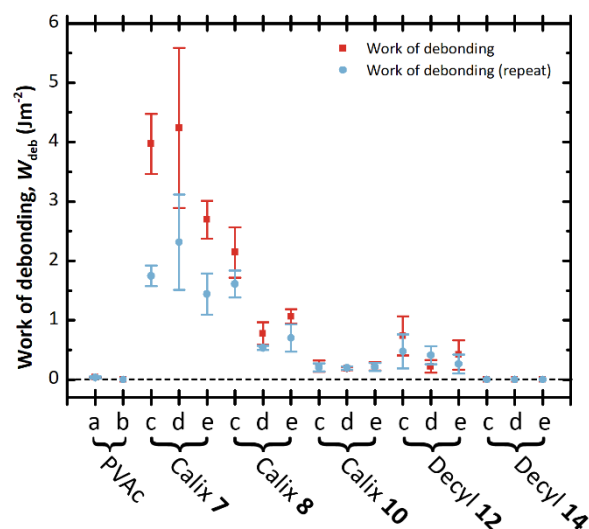


**Figure 8:** Work of debonding of PVAc, calix[4]resorcinarene adhesives, and decyl controls. Measurements were conducted in pH6 Milli-Q water using pDEAEMA and DN pMAA-pOEGMA hydrogels. The applied load is 0.5 N with a contact time of 2 min. The speed of approach and retraction of the hydrogel probe is 50 mm min<sup>-1</sup>. a) Adhesion with DN pMAA-pOEGMA hydrogel. b) Adhesion with pDEAEMA hydrogel. c) As-deposited samples. d) 100 °C Post-baked samples. e) H<sub>2</sub>O sonicated samples.

The values obtained for the work of debonding and the maximum stress are plotted with the data reported previously<sup>14,16</sup> in Figure 9. In addition to the values recorded at an applied load of 0.5 N, values were also recorded at applied loads of 0.1 N and 2 N. The stresses measured are not large, and are similar to those reported by La Spina et al.<sup>14</sup> The values for the work of debonding are greater than those obtained for pDMAEMA<sup>14</sup> but less than those reported for pDEAEMA.<sup>16</sup> However, the results reported by Alfhaid et al.<sup>16</sup> were obtained at much larger stresses, where some plastic deformation is likely to have occurred.<sup>43</sup>

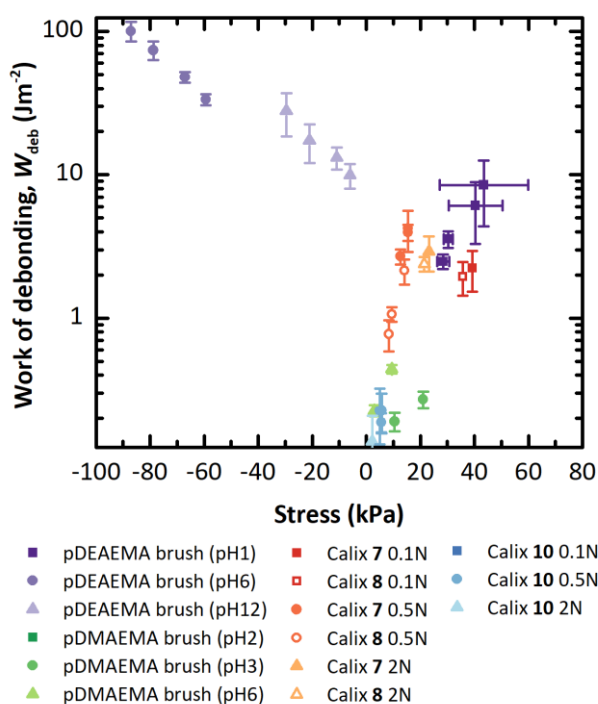


**Figure 9:** Comparison of work of debonding and stress, including data from grafted-from pDEAEMA<sup>16</sup> and pDMAEMA<sup>14</sup> brushes. Calixarene-based adhesion data were recorded at applied loads of 0.1 N, 0.5 N, and 2 N.

From this comparison, it can be seen that the adhesion data obtained are consistent with other polyelectrolyte brush systems. These polyelectrolyte brush systems do not give the strongest adhesive bonds, but the data obtained using

calixarene-polyelectrolyte brushes are similar to those for brushes attached to the surface using a chemical bond. This shows that the calixarene is anchoring the brush to the surface as efficiently as a chemical bond in this system, and that the adhesion has not been adversely affected by replacing a chemically tethered grafted-from brush, which is hard to produce, with a physically adsorbed grafted-to brush, which is comparatively easier to deposit. Calixarene-polyelectrolyte brushes provide access to the same adhesive mechanisms as the grafted-from brush, but via a grafting-to technique, meaning they no longer have to be prepared *in situ*. The amphiphilic nature of the calixarene-polyelectrolyte system allows for self-organization of the calixarene on the water surface during deposition, which, in turn, generates a densely grafted monolayer of adhesive when transferred to a surface. This *ex situ* nature gives the potential for their use in applications previously unavailable due to the limitations of surface preparation, thus enabling a possible new route to water-based adhesives with a wide variety of materials.

## Conclusions

These experiments provide a first step towards creating a water-based adhesive that could be practicable in real-world environments for switchable applications. To achieve this, a grafting-to method was used whereby a pre-synthesized polymer was deposited on a surface without the need for a more complicated grafting-from method. These experiments showed that this approach holds promise because grafting-to methods require less stringent control of the surfaces to be adhered. In this work a Langmuir trough was used for self-organization of the calixarene on the water surface during deposition, whilst this would not be practical in general use it allows for controlled evaluation and therefore demonstrates the potential of grafted-to adhesives. Furthermore, the other (oppositely charged) surface is a standard polymer gel, which represents only one class of real-world surface that may be adhered. Methodologies could be tailored to different kinds of surfaces by appropriately functionalizing the resorcinarene so a grafting-to method for reversible and repeatable adhesion is viable. The deposition of monolayers from an aqueous surface would work well on either very flat or conformable surfaces. Rough surfaces may leave insufficient contact points for sufficiently strong adhesion.

## Supporting Information

Additional experimental details, synthesis of the decyl control compounds, and NMR spectra. This material is available free of charge via the Internet at <http://pubs.acs.org>.

## Author Information

### Corresponding Author

[william.seddon@infineum.com](mailto:william.seddon@infineum.com)

### Present addresses

WDS: Infineum UK Ltd., P.O. Box 1, Milton Hill, Abingdon, Oxfordshire, OX13 6BB, UK

LA: Department of Physics, College of Science, University of Ha'il, Hail, Saudi Arabia.

MG: School of Engineering, Newcastle University, Merz Court, Newcastle NE1 7RU, UK

## Notes

The authors declare no competing financial interest.

## Acknowledgements

A doctoral scholarship was provided for WDS by the Engineering and Physical Sciences Research Council (EPSRC) through the Centre for Doctoral Training in Molecular Engineering of the Universities of Sheffield and Leeds. The Ministry of Education of the Kingdom of Saudi Arabia represented by Ha'il University is acknowledged for a PhD scholarship for LA.

## References

- (1) Ahuja, B. B.; Vigalok, A. Fluorescent Calixarene Scaffolds for NO Detection in Protic Media. *Angew. Chemie Int. Ed.* **2019**, *58*, 2774–2778.
- (2) Zhu, Y.; Rebek Jr, J.; Yu, Y. Cyclizations catalyzed inside a hexameric resorcinarene capsule. *Chem. Commun.* **2019**, *55*, 3573–3577.
- (3) Hou, Y.; Chai, D.; Li, B.; Pang, H.; Ma, H.; Wang, X.; Tan, L. Polyoxometalate-Incorporated Metallacalixarene@Graphene Composite Electrodes for High-Performance Supercapacitors. *ACS Appl. Mater. Interfaces* **2019**, *11*, 20845–20853.
- (4) Barba-Bon, A.; Pan, Y.-C.; Biedermann, F.; Guo, D.-S.; Nau, W. M.; Hennig, A. Fluorescence Monitoring of Peptide Transport Pathways into Large and Giant Vesicles by Supramolecular Host–Dye Reporter Pairs. *J. Am. Chem. Soc.* **2019**, *141*, 20137–20145.
- (5) Skala, L. P.; Yang, A.; Klemes, M. J.; Xiao, L.; Dichtel, W. R. Resorcinarene Cavitand Polymers for the Remediation of Halomethanes and 1,4-Dioxane. *J. Am. Chem. Soc.* **2019**, *141*, 13315–13319.
- (6) Blond, P.; Mattiuzzi, A.; Valkenier, H.; Troian-Gautier, L.; Bergamini, J.-F.; Doneux, T.; Goormaghtigh, E.; Raussens, V.; Jabin, I. Grafting of Oligo(ethylene glycol)-Functionalized Calix[4]arene-Tetradiazonium Salts for Antifouling Germanium and Gold Surfaces. *Langmuir* **2018**, *34*, 6021–6027.
- (7) Behboodi-Sadabad, F.; Trouillet, V.; Welle, A.; Messersmith, P. B.; Levkin, P. A. Surface Functionalization and Patterning by Multifunctional Resorcinarenes. *ACS Appl. Mater. Interfaces* **2018**, *10*, 39268–39278.
- (8) Yabushita, M.; Grosso-Giordano, N. A.; Fukuoka, A.; Katz, A. Selective Sequestration of Aromatics from Aqueous Mixtures with Sugars by Hydrophobic Molecular Calixarene Cavities Grafted on Silica. *ACS Appl. Mater. Interfaces* **2018**, *10*, 39670–39678.
- (9) Dinda, S. K.; Althaf Hussain, M.; Upadhyay, A.; Rao, C. P. Supramolecular Sensing of 2,4,6-Trinitrophenol by a Tetrapyrenyl Conjugate of Calix[4]arene: Applicability in Solution, in Solid State, and on the Strips of Cellulose and Silica Gel and the Image Processing by a Cellular Phone. *ACS Omega* **2019**, *4*, 17060–17071.
- (10) Español, E.; Villamil, M. Calixarenes: Generalities and Their Role in Improving the Solubility, Biocompatibility, Stability, Bioavailability, Detection, and Transport of Biomolecules. *Biomolecules* **2019**, *9*, 90.
- (11) Ferreira, J. F.; Bagatin, I. A. A Cr(VI) selective probe based on a quinoline-amide calix[4]arene. *Spectrochim. Acta Part A Mol. Biomol. Spectrosc.* **2018**, *189*, 44–50.
- (12) Wang, T.; Canetta, E.; Weerakkody, T. G.; Keddie, J. L.; Rivas, U. pH dependence of the properties of waterborne pressure-sensitive adhesives containing acrylic acid. *ACS Appl. Mater. Interfaces* **2009**, *1*, 631–639.
- (13) Nolte, A. J.; Chung, J. Y.; Walker, M. L.; Stafford, C. M. In situ adhesion measurements utilizing layer-by-layer functionalized surfaces. *ACS Appl. Mater. Interfaces* **2009**, *1*, 373–380.

- (14) La Spina, R.; Tomlinson, M. R.; Ruiz-Pérez, L.; Chiche, A.; Langridge, S.; Geoghegan, M. Controlling Network–Brush Interactions to Achieve Switchable Adhesion. *Angew. Chemie Int. Ed.* **2007**, *46*, 6460–6463.
- (15) Alfheid, L.; Seddon, W. D.; Williams, N. H.; Geoghegan, M. Double-network hydrogels improve pH-switchable adhesion. *Soft Matter* **2016**, *12*, 5022–5028.
- (16) Alfheid, L.; La Spina, R.; Tomlinson, M. R.; Hall, A. R.; Seddon, W. D.; Williams, N. H.; Cousin, F.; Gorb, S.; Geoghegan, M. Adhesion between oppositely charged polyelectrolytes. *J. Adhes.* **2018**, *94*, 58–76.
- (17) Gong, J. P. Why are double network hydrogels so tough? *Soft Matter* **2010**, *6*, 2583–2590.
- (18) Kobayashi, M.; Terada, M.; Takahara, A. Reversible adhesive-free nanoscale adhesion utilizing oppositely charged polyelectrolyte brushes. *Soft Matter* **2011**, *7*, 5717–5722.
- (19) Sudre, G.; Olanier, L.; Tran, Y.; Hourdet, D.; Creton, C. Reversible adhesion between a hydrogel and a polymer brush. *Soft Matter* **2012**, *8*, 8184.
- (20) Raftari, M.; Zhang, Z. J.; Carter, S. R.; Leggett, G. J.; Geoghegan, M. Nanoscale Contact Mechanics between Two Grafted Polyelectrolyte Surfaces. *Macromolecules* **2015**, *48*, 6272–6279.
- (21) Weir, M. P.; Parnell, A. J. Water Soluble Responsive Polymer Brushes. *Polymers* **2011**, *3*, 2107–2132.
- (22) Li, B.; Whalen, J. J.; Humayun, M. S.; Thompson, M. E. Reversible Bioadhesives Using Tannic Acid Primed Thermally-Responsive Polymers. *Adv. Funct. Mater.* **2020**, *30*, 1907478.
- (23) Wang, J.; Chen, X.-Y.; Zhao, Y.; Yang, Y.; Wang, W.; Wu, C.; Yang, B.; Zhang, Z.; Zhang, L.; Liu, Y.; Du, X.; Li, W.; Qiu, L.; Jiang, P.; Mou, X.-Z.; Li, Y.-Q. pH-Switchable Antimicrobial Nanofiber Networks of Hydrogel Eradicate Biofilm and Rescue Stalled Healing in Chronic Wounds. *ACS Nano* **2019**, *13*, 11686–11697.
- (24) Zhou, Y.; Chen, M.; Ban, Q.; Zhang, Z.; Shuang, S.; Koynov, K.; Butt, H.-J.; Kong, J.; Wu, S. Light-Switchable Polymer Adhesive Based on Photoinduced Reversible Solid-to-Liquid Transitions. *ACS Macro Lett.* **2019**, *8*, 968–972.
- (25) Banea, M. D.; Da Silva, L. F. M.; Carbas, R. J. C.; Cavalcanti, D. K. .; De Souza, L. F. G. The effect of environment and fatigue loading on the behaviour of TEPs-modified adhesives. *J. Adhes.* **2020**, *96*, 423–436.
- (26) Yu, L.; Peng, R.; Rivers, G.; Zhang, C.; Si, P.; Zhao, B. Multifunctional liquid crystal polymer network soft actuators. *J. Mater. Chem. A* **2020**, *8*, 3390–3396.
- (27) Xing, S.; Wang, P.; Liu, S.; Xu, Y.; Zheng, R.; Deng, Z.; Peng, Z.; Li, J.; Wu, Y.; Liu, L. A shape-memory soft actuator integrated with reversible electric/moisture actuating and strain sensing. *Compos. Sci. Technol.* **2020**, *193*, 108133.
- (28) Mumladze, T.; Yousef, S.; Tatariants, M.; Kriūkienė, R.; Makarevicius, V.; Lukošūtė, S.-I.; Bendikiene, R.; Denafas, G. Sustainable approach to recycling of multilayer flexible packaging using switchable hydrophilicity solvents. *Green Chem.* **2018**, *20*, 3604–3618.
- (29) Jeong, H. E.; Kwak, M. K.; Suh, K. Y. Stretchable, Adhesion-Tunable Dry Adhesive by Surface Wrinkling. *Langmuir* **2010**, *26*, 2223–2226.
- (30) Ferahian, A.; Hohl, D. K.; Weder, C.; Montero de Espinosa, L. Bonding and Debonding on Demand with

- Temperature and Light Responsive Supramolecular Polymers. *Macromol. Mater. Eng.* **2019**, *304*, 1900161.
- (31) Shahsavan, H.; Salili, S. M.; Jáklí, A.; Zhao, B. Thermally Active Liquid Crystal Network Gripper Mimicking the Self-Peeling of Gecko Toe Pads. *Adv. Mater.* **2017**, *29*, 1604021.
- (32) Li, M.; Dai, Q.; Jiao, Q.; Huang, W.; Wang, X. Magnetically stimulating capillary effect for reversible wet adhesions. *Soft Matter* **2019**, *15*, 2817–2825.
- (33) Heng, L.; Guo, T.; Wang, B.; Fan, L.-Z.; Jiang, L. In situ electric-driven reversible switching of water-droplet adhesion on a superhydrophobic surface. *J. Mater. Chem. A* **2015**, *3*, 23699–23706.
- (34) Kim, H. J.; Paquin, L.; Barney, C. W.; So, S.; Chen, B.; Suo, Z.; Crosby, A. J.; Hayward, R. C. Low-Voltage Reversible Electroadhesion of Ionoelastomer Junctions. *Adv. Mater.* **2020**, *32*, 2000600.
- (35) Shui, L.; Jia, L.; Li, H.; Guo, J.; Guo, Z.; Liu, Y.; Liu, Z.; Chen, X. Rapid and continuous regulating adhesion strength by mechanical micro-vibration. *Nat. Commun.* **2020**, *11*, 1583.
- (36) Hwang, D.-G.; Trent, K.; Bartlett, M. D. Kirigami-Inspired Structures for Smart Adhesion. *ACS Appl. Mater. Interfaces* **2018**, *10*, 6747–6754.
- (37) Wang, Y.; Tian, H.; Shao, J.; Sameoto, D.; Li, X.; Wang, L.; Hu, H.; Ding, Y.; Lu, B. Switchable Dry Adhesion with Step-like Micropillars and Controllable Interfacial Contact. *ACS Appl. Mater. Interfaces* **2016**, *8*, 10029–10037.
- (38) Wang, Z.; Guo, L.; Xiao, H.; Cong, H.; Wang, S. A reversible underwater glue based on photo- and thermo-responsive dynamic covalent bonds. *Mater. Horizons* **2020**, *7*, 282–288.
- (39) Wang, X.; Tan, D.; Hu, S.; Li, Q.; Yang, B.; Shi, Z.; Das, R.; Xu, X.; Wu, Z.-S.; Xue, L. Reversible Adhesion via Light-Regulated Conformations of Rubber Chains. *ACS Appl. Mater. Interfaces* **2019**, *11*, 46337–46343.
- (40) Yu, Y.; Kieviet, B. D.; Kutnyanszky, E.; Vancso, G. J.; de Beer, S. Cosolvency-Induced Switching of the Adhesion between Poly(methyl methacrylate) Brushes. *ACS Macro Lett.* **2015**, *4*, 75–79.
- (41) Chiang, P. J.; Tang, G.; Kwon, I. S.; Eristoff, S.; Bettinger, C. J. Reversible Chemo-Topographic Control of Adhesion in Polydopamine Nanomembranes. *Macromol. Mater. Eng.* **2018**, *303*, 1–8.
- (42) Park, K. H.; Seong, K.-Y.; Yang, S. Y.; Seo, S. Advances in medical adhesives inspired by aquatic organisms' adhesion. *Biomater. Res.* **2017**, *21*, 16.
- (43) Alfheid, L.; Williams, N. H.; Geoghegan, M. Adhesion between oppositely charged polyelectrolytes in salt solution. *J. Appl. Polym. Sci.* **2020**, No. February, 49130.
- (44) Raftari, M.; Zhang, Z. J.; Carter, S. R.; Leggett, G. J.; Geoghegan, M. Salt Dependence of the Tribological Properties of a Surface-Grafted Weak Polycation in Aqueous Solution. *Tribol. Lett.* **2018**, *66*, 11.
- (45) Keller, R. N.; Wrcoff, H. D.; Marchi, L. E. Copper(I) Chloride. In *Inorganic Syntheses, Volume II*; W. Conard Fernelius, Ed.; McGraw-Hill Book Company, Inc.: Hoboken, NJ, USA, 1946; pp 1–4.
- (46) Fairfull-Smith, K.; Redon, P. M. J.; Haycock, J. W.; Williams, N. H. Monofunctionalised resorcinarenes. *Tetrahedron Lett.* **2007**, *48*, 1317–1319.
- (47) Ito, H.; Nakayama, T.; Sherwood, M.; Miller, D.; Ueda, M. Characterization and lithographic application of

- calix[4]resorcinarene derivatives. *Chem. Mater.* **2008**, *20*, 341–356.
- (48) Hansen, M. M.; Riggs, J. R. A novel protecting group for hindered phenols. *Tetrahedron Lett.* **1998**, *39*, 2705–2706.
- (49) Ye, M.; Zhang, D.; Han, L.; Tejada, J.; Ortiz, C. Synthesis, preparation, and conformation of stimulus-responsive end-grafted poly(methacrylic acid-g-ethylene glycol) layers. *Soft Matter* **2006**, *2*, 243–256.
- (50) Wei, X.; Gong, X.; Ngai, T. Investigating interactions between cationic particles and polyelectrolyte brushes with Total Internal Reflection Microscopy (TIRM). *Polym. Chem.* **2013**, *4*, 4356–4365.
- (51) Heeb, R.; Bielecki, R. M.; Lee, S.; Spencer, N. D. Room-temperature, aqueous-phase fabrication of poly(methacrylic acid) brushes by UV-LED-induced, controlled radical polymerization with high selectivity for surface-bound species. *Macromolecules* **2009**, *42*, 9124–9132.
- (52) Spruijt, E.; Leermakers, F. A. M.; Fokkink, R.; Schweins, R.; Van Well, A. A.; Cohen Stuart, M. A.; Van Der Gucht, J. Structure and dynamics of polyelectrolyte complex coacervates studied by scattering of neutrons, X-rays, and light. *Macromolecules* **2013**, *46*, 4596–4605.
- (53) Bickel, T.; Jeppesen, C.; Marques, C. M. Local entropic effects of polymers grafted to soft interfaces. *Eur. Phys. J. E* **2001**, *4*, 33–43.
- (54) Sanjuan, S.; Perrin, P.; Pantoustier, N.; Tran, Y. Synthesis and swelling behavior of pH-responsive polybase brushes. *Langmuir* **2007**, *23*, 5769–5778.
- (55) Brittain, W. J.; Minko, S. A structural definition of polymer brushes. *J. Polym. Sci. Part A Polym. Chem.* **2007**, *45*, 3505–3512.
- (56) Collyer, S. D.; Davis, F.; Lucke, A.; Stirling, C. J. M.; Higson, S. P. J. The electrochemistry of the ferri/ferrocyanide couple at a calix[4]resorcinarenetetrathiol-modified gold electrode as a study of novel electrode modifying coatings for use within electro-analytical sensors. *J. Electroanal. Chem.* **2003**, *549*, 119–127.
- (57) Creton, C.; Ciccotti, M. Fracture and adhesion of soft materials: a review. *Reports Prog. Phys.* **2016**, *79*, 046601.

For Table of Contents Only

